

## PAPER

# A Novel Validation Study of a Wrist Orthosis for the Objective Evaluation of Rigidity in Parkinson's Disease

Caio Tonus Ribeiro<sup>1</sup>, Daniel Hilário da Silva<sup>1,2</sup>(✉), Leandro Rodrigues da Silva Souza<sup>1,3</sup>, José Renato Munari Nardo<sup>1</sup>, Adriano Alves Pereira<sup>1,4</sup>

<sup>1</sup>Programa de Pós-Graduação em Engenharia Biomédica, Uberlândia, Brasil

<sup>2</sup>Instituto Federal Goiano – Campus Cristalina, Cristalina, Brasil

<sup>3</sup>Instituto Federal Goiano – Campus Rio Verde, Rio Verde, Brasil

<sup>4</sup>Faculdade de Engenharia Elétrica, Uberlândia, Brasil

[daniel.hilario@ifgoiano.edu.br](mailto:daniel.hilario@ifgoiano.edu.br)

## ABSTRACT

Parkinson's disease (PD) is a neurological condition affecting millions, marked by mobility issues and characterized by motor and non-motor symptoms, including tremors, bradykinesia, postural instability, and rigidity. Diagnosis often relies on subjective assessments such as the Movement Disorder Society Unified PD Rating Scale (MDS-UPDRS). This study focuses on validating a wrist orthosis designed to quantify rigidity in PD patients objectively. Developed at the Center for Innovation and Technological Evaluation in Health (NIATS), the orthosis integrates a Faulhaber linear motor (LM 2070-080-11) and microcontroller (MCLM 3006 S RS). Calibration experiments, including varied mass assessments, established the orthosis's reliability. Results indicated a newly calculated force constant of 14.28 N/A, 18.49% higher than the manufacturer's value, with a strong Pearson correlation coefficient (0.9997189). The orthosis detected masses ranging from 39.07 to 812.64 grams without yielding. Angular displacement calibration, utilizing a GP10 goniometer and Myosystem-Br1 software, demonstrated linearity, supported by Pearson coefficients of 0.9995091 and 0.9995259. These findings underscore the orthosis's potential as a reliable tool for measuring rigidity in PD patients, promising advancements in physiotherapy and disease monitoring.

## KEYWORDS

Parkinson's disease (PD), orthosis, objective quantification, rigidity, physiotherapy

## 1 INTRODUCTION

Parkinson's disease (PD) is a progressive neurological pathology that impacts individual mobility and affects millions of people worldwide, with a higher prevalence in men [1], [2]. It is also the second most common neurodegenerative disease after Alzheimer's disease [3], presenting various motor and non-motor signs and symptoms; non-motor ones include cognitive or neurobehavioral abnormalities, sleep disorders, and pain, among others. [2] Motor symptoms include four cardinal

Ribeiro, C.T., da Silva, D.H., da Silva Souza, L.R., Nardo, J.R.M., Pereira, A.A. (2024). A Novel Validation Study of a Wrist Orthosis for the Objective Evaluation of Rigidity in Parkinson's Disease. *International Journal of Online and Biomedical Engineering (iJOE)*, 20(12), pp. 90–108. <https://doi.org/10.3991/ijoe.v20i12.50429>

Article submitted 2024-06-05. Revision uploaded 2024-07-18. Final acceptance 2024-07-19.

© 2024 by the authors of this article. Published under CC-BY.

features: bradykinesia, resting tremor, muscle rigidity, and postural instability [1], with rigidity being the focus of this work.

A PD diagnosis is made through clinical analysis if the patient presents at least two of the four cardinal signs and symptoms, considering the individual's medical and family history. The gold standard for assessment is the Unified PD Rating Scale (UPDRS), optimized by the Movement Disorder Society (MDS): the MDS-UPDRS [4]. This scale helps evaluate disease progression from zero (normal) to four (unable to perform the task), divided into four parts: mood and behavior assessments (part I), daily living activities (part II), motor abilities (part III), and motor complications (part IV).

The most frequently used treatments to alleviate PD signs and symptoms are medications (such as levodopa or dopaminergic drugs) or surgical procedures, such as Deep Brain Stimulation (DBS) [1], [2]. Despite the adverse effects of medications and the invasive nature of surgical intervention, physiotherapeutic procedures have shown growing relevance and validity in treating PD symptoms, whether these procedures are associated with medication or surgery or not [5], [6]. Robotic technologies have been employed in the rehabilitation of upper and lower limbs in recent years, demonstrating potential improvements in therapy outcomes [7], [8], [9], and [10]. Although tremor is the most well-known cardinal symptom in PD individuals, the symptoms that most affect motor ability are gait alteration and rigidity.

Rigidity is defined as resistance—often associated with tremors—present throughout the passive movement of a limb (flexion, extension, or rotation) [2]. Individuals affected by rigidity have compromised mobility, which leads to difficulties in daily activities and a reduction in their quality of life [11], [12]. The rigidity can be evaluated by item III of the MDS-UPDRS, which assesses various aspects such as speech, rigidity, agility of the lower and upper limbs, and gait, among others; however, it is a subjective evaluation. Thus, there is a need for a methodology that allows an objective evaluation of rigidity in PD patients. Various approaches have been proposed over the years, but objective quantification of rigidity remains a challenge [13].

Some proposed methodologies for objective rigidity measurement use inertial measurement units (IMUs), employing accelerometers, gyroscopes, magnetometers, and potentiometers. Others use electromyography, myotonometry, or elastography data to analyze rigidity during muscular activation in flexion and extension movements [14], [15]. Another approach involves using servomotors for passive joint movement while collecting other signals [16], [17]. Objective rigidity measurements can be observed in various joints. The wrist, however, plays a significant role in daily life activities such as opening a door, answering the phone, or eating, making wrist flexion and extension movements crucial for better quality-of-life in PD individuals [18], [19].

Given the need for a non-subjective method to aid in rigidity quantification in PD patients, the instrumentation of a wrist orthosis is proposed. This orthosis consists of a linear servomotor and inherent current and position sensors, allowing the estimation of the force exerted by the motor using a force constant provided by the manufacturer, though it requires calibration for the intended use. Signals are extracted to analyze the force needed for the orthosis to perform wrist flexion and extension movements.

Thus, this study's relevance is emphasized in supporting the physiotherapy field, as accurate DP stage quantification can provide valuable information for the treatment and monitoring of affected individuals. Furthermore, a precise diagnosis

followed by appropriate treatment and monitoring can improve the quality of life for individuals with PD. The orthosis instrumentation aims to enable future classification of healthy and PD patients through characteristics extracted from current signals, linear displacement of the actuator rod, and angular displacement analyzed in this research.

## 2 MATERIALS AND METHODS

### 2.1 General description of the orthosis

The active wrist orthosis (AWO) used in this study was developed at NIATS [20], [21]. It weighs 850 grams and comprises an actuator, a linear servomotor LM 2070-080-11 (Faulhaber, Germany) [22], and a high-precision controller MCLM 3006 S RS (Faulhaber, Germany) [23]. The orthosis is registered with the National Institute of Industrial Property (INPI) under patent number BR10 2014 023282 6. The orthosis and its components are shown in Figure 1.

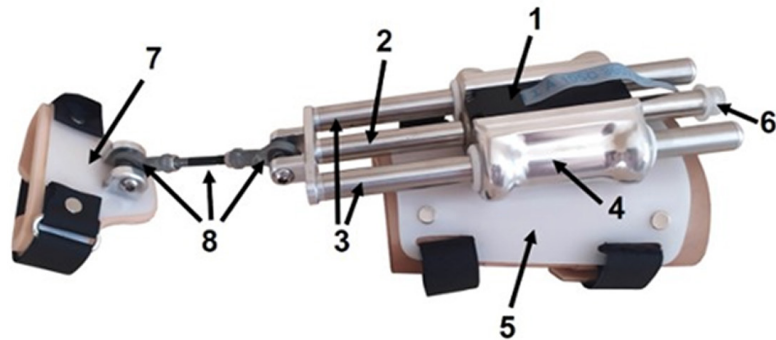


**Fig. 1.** Identification of the parts that make up the orthosis, adapted from [20]

The components are related as follows: (1) actuator, (2) actuator cylindrical shaft, (3) auxiliary cylindrical shafts developed to provide more stability to the actuator's movement, (4) actuator case, (5) structure attached to the forearm, (6) displacement limiter used for safety, (7) structure that attaches to the hand, and (8) spherical joints that allow multidimensional hand movement.

To instrument the orthosis for quantifying rigidity in patients with PD, a method is needed to evaluate the force and current required for wrist flexion and extension movements, as well as the angular displacement caused by the actuator's movement. This will confirm the viability of the AWO as an objective tool for quantifying rigidity.

### 2.2 Actuator, controller, and software

**Actuator.** The LM 2070-080-11 actuator is a brushless DC motor, meaning it lacks brushes and thus relies on electronic control rather than a mechanical system to manage electrical current. Hall effect sensors are used to detect the position and speed of the rod, sending this information to the MCLM 3006 S RS controller, which manages these values. The actuator's specifications can be found on the technical

manual for the LM 2070-080-11, available on the manufacturer's website, at a temperature of 22 °C and a supply voltage of 12 volts [22], [23].

The total length of the rod is 182 mm; however, since the fixed part of the actuator is 74 mm long, approximately 54 mm remain on each side of the rod. With the addition of end fixings, there is a safety margin of 14 mm, leaving 40 mm for movement on each side, resulting in a total maximum displacement of 80 mm, as shown in Figure 2.

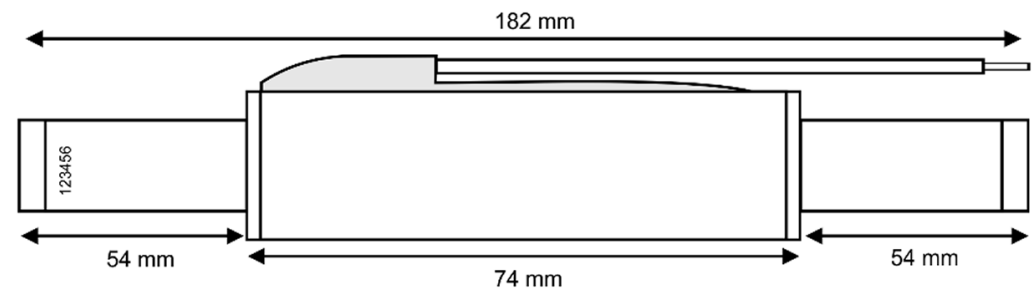


Fig. 2. Actuator measurements

This total maximum displacement of 80 mm is divided into 10,000 increments, with 5,000 increments on each side of the fixed part of the motor and 40 mm on each side. In this study, positions such as 5,000 and  $-5,000$  refer to the rod's displacement, with the positive side representing one direction and the negative side the opposite, with zero being the initial position of the rod. Therefore, each increment corresponds to a movement of 0.008 mm. Considering the actuator's accuracy of 0.3 mm, there may be a variance of up to 37.5 increments, representing a possible error of 0.375% relative to the expected position over 10,000 increments. Similarly, the motor's repeatability or precision is 0.06 mm, indicating a possible discrepancy of up to 7.5 increments when selecting the same position twice, equivalent to a 0.075% error relative to the expected position, again considering 10,000 increments. To ensure optimal performance of the selected actuator, a capable control device is necessary.

**Controller.** The MCLM 3006 S RS is a highly dynamic position controller that manages linear motors with analog hall sensors, controlling position and speed through the current supplied to the actuator. This controller version includes memory for saving pre-established parameters and an RS232 port for communication with the data-receiving device, in this case, a computer. This microcontroller was selected based on the manufacturer's usage recommendation. It offers overload protection for both the motor and the controller itself, enabling precise control of the actuator rod's position, speed, and acceleration.

Communication between the software and the controller is achieved through ASCII standard commands sent via the serial port, in this case, using the motion manager terminal or a file containing instructions sent to the controller. This occurs via RS232 using a serial port and an RS232-USB converter cable, which sends commands to the controller to execute and capture information from the motor's hall sensors, transmitting it back to the motion manager. All information is transmitted to the computer at 38,400 bits/s. It is also possible to graphically analyze the values obtained from the sensors, observe the signals, and save them for later analysis. This graphical interface provides the current consumed by the motor and the rod displacement values.

**Software.** To analyze the desired parameters, FAULHABER motion manager 6 (Faulhaber, Germany), version 6.9.0, was used, as shown in Figures 3 and 4. This free software is developed and distributed by the manufacturer of the other components used, selected for its ease of use with the MCLM 3006 S RS controller [23]. Motion manager can also be used to obtain the best configuration and control parameters for the linear motor, such as the integral, differential, or proportional terms of position or velocity in Figure 3, the maximum displacement limits of the movable rod, or even place the rod precisely in the middle of the actuator.

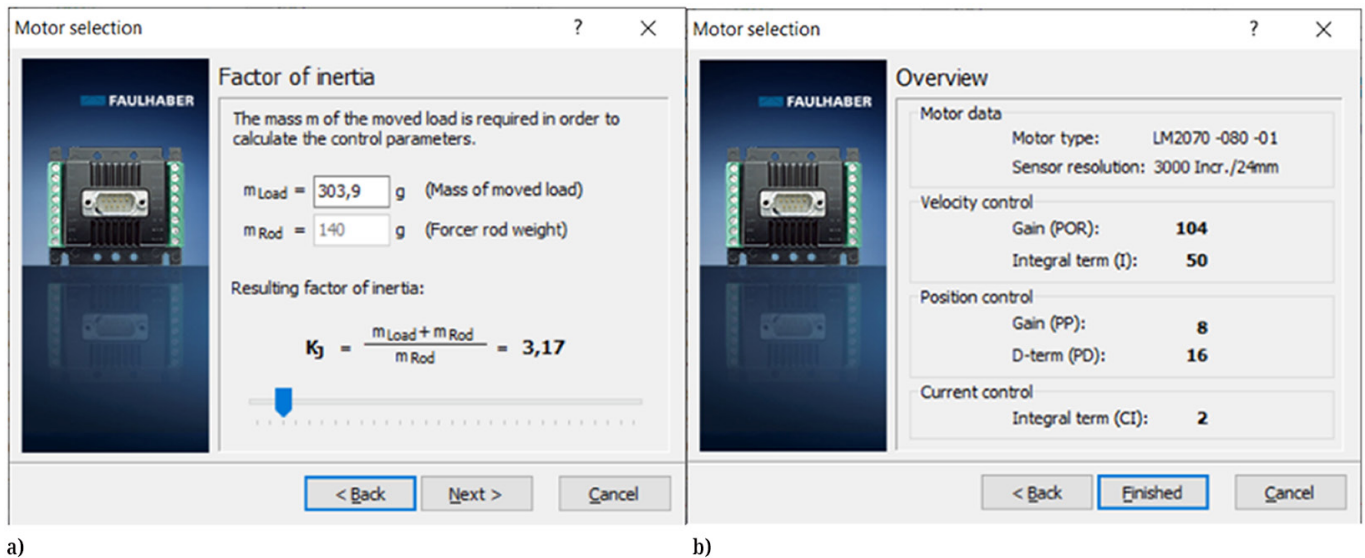


Fig. 3. PID (proportional, integral and derivative) optimization screen

In Figure 3a, the optimization of the PI (proportional and integral) parameters for speed and the PD (proportional and differential) parameters for position, as well as the integral current parameter, are shown. Initially, the load that the motor will move, “Load,” is selected. The software calculates the resulting inertia factor and obtains the parameters shown in Figure 3b. It is important to note that if the load mass changes, these parameters need to be re-optimized. After optimizing the controller, the hall sensors of the motor need to be calibrated using the tools tab in motion manager. Calibration ensures precise control of position and speed. In Motion Manager 6, it is possible to set the rod’s positions as well as the speed at which it will move. After the PID calibration, the rod is automatically set to position 0, allowing for an even more precise measurement.

### 2.3 Considered protocols

**Protocol for evaluating the current consumed by the orthosis.** The actuator used in the orthosis consumes electrical current to move the rod to a certain position at a certain speed. As mentioned earlier, the actuator has hall effect sensors, which react when subjected to a magnetic field, sending information such as the current position of the rod or the current consumed by the motor. Therefore, due to the presence of internal sensors, it is possible to verify the current consumed through the hall effect sensors and the graphical interface of Motion Manager 6, as seen in Figure 4. Note the scale of both the rod’s actual position and the motor’s current consumption.

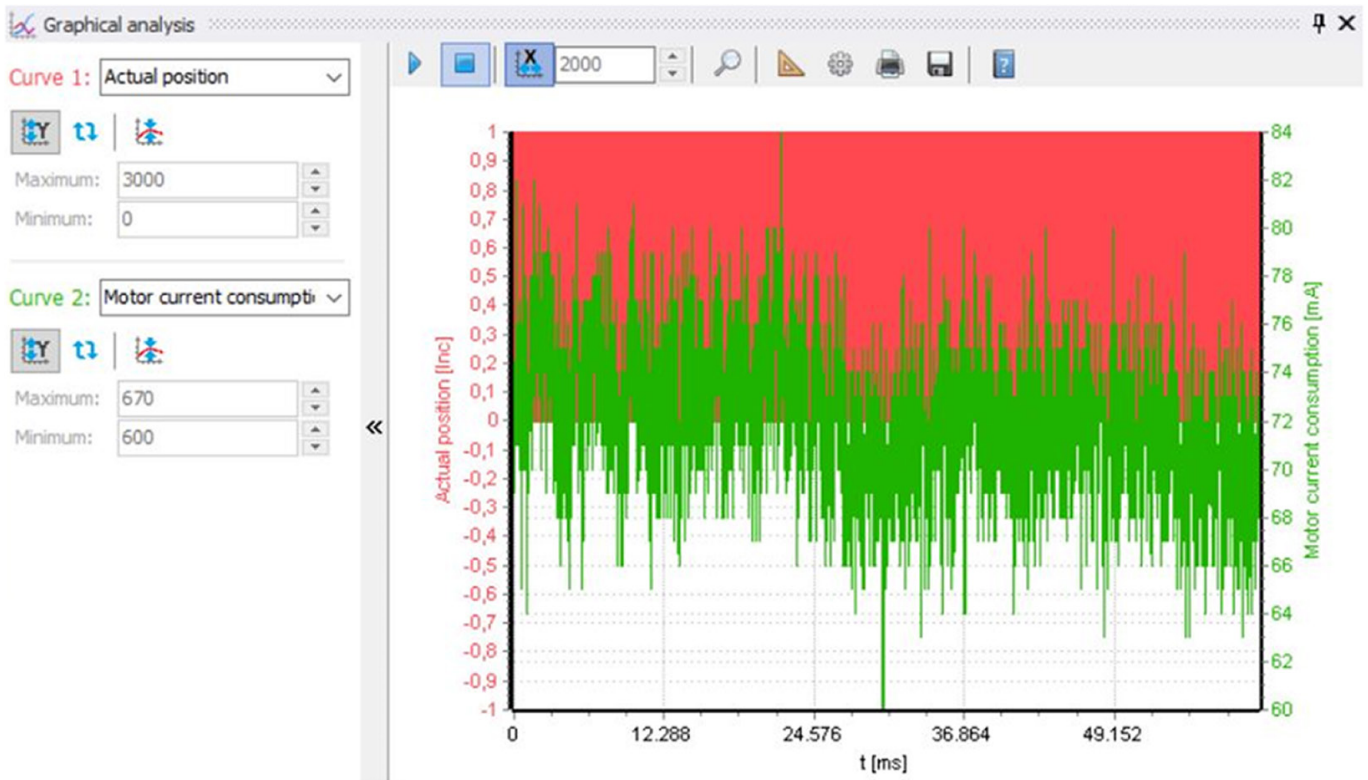


Fig. 4. Motion Manager 6 graphical analysis interface

**Protocol for calibrating the force exerted by the orthosis.** This approach, which was straightforward and required no additional calibrations, yielded satisfactory results for this study. It involved using a pulley, a negligible-mass rope (0.185 g), and different masses. The various evaluated masses were attached by a hook to the rope, which was in turn connected to the actuator's movable rod, fixed to the table with non-magnetic clamps. The masses were situated on the "negative" side of the rod for reference. For each different mass placed, the PID parameters were optimized in Figure 3, and the hall sensors were calibrated for the mass. Before hanging the mass on the rope, the motor was moved to the 0 position (center). The experiment setup was then performed, and the current signal was captured for 60 seconds at a sampling frequency of 166.67 Hz. The flowchart explaining this process is shown in Figure 5.

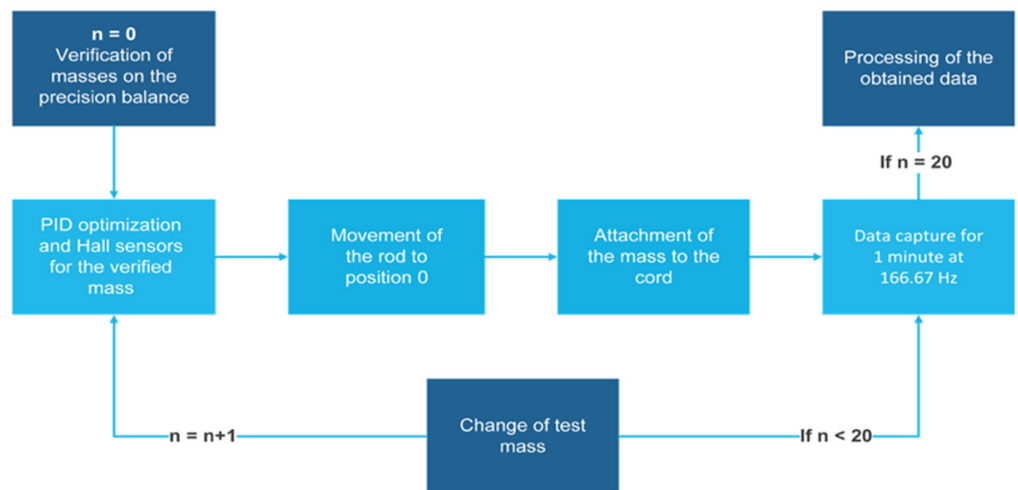


Fig. 5. Flowchart of the data collection protocol

This signal was then processed in RStudio software, where a 4th-order 1 Hz Butterworth low-pass filter was applied to remove unwanted frequencies. After this preprocessing, the mean current value, given in A for each mass, was calculated. The force constant provided by the manufacturer is 11.64 N/A, which was used to calculate the force, given in N, that the motor exerts to maintain the system in equilibrium. The apparent measured mass was then calculated by dividing the force value by 9.78 m/s<sup>2</sup> (a value calculated by the Institute of Geography at the Federal University of Uberlândia on December 7, 2020, by the Center for Geodesy Studies, CENEGEO) [24]. The experiment's setup can be seen in Figure 6, and the practical setup in Figure 7.

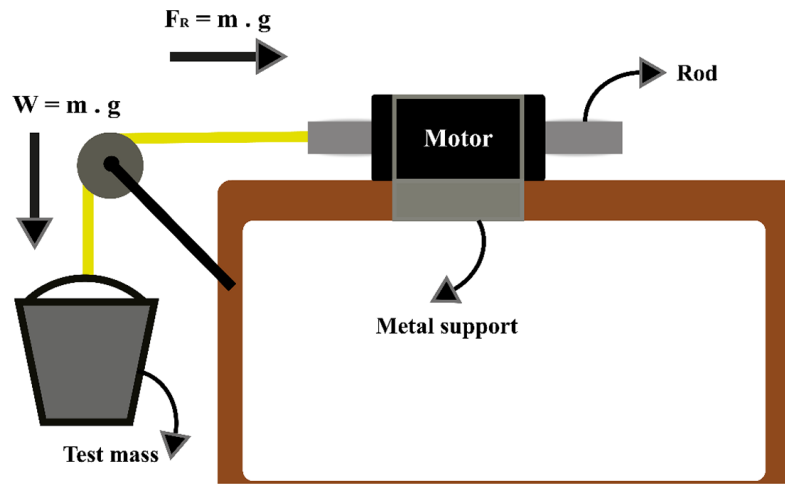


Fig. 6. Initial outline of the approach utilized

In Figure 7, two views are provided: the upper (left) and side (right) views, showing the mass strapped to the actuator's rod through a thin string of insignificant mass (0.185 g) compared to the masses used in the experiment.



Fig. 7. Practical setup of the proposed approach

These masses comprise five solid metallic cylinders (M1 through M5), five solid plastic cylinders (P1 through P5), two hollow metallic cylinders (O1 and O2), and two plastic cups where the masses were put into (C1 and C2) and were weighted on

a precision balance. Mass C1 considers the weight of the hook used to strap the test masses. (refer to Table 1).

**Table 1.** Test masses used to calibrate the force exerted by the motor

Test Mass	Mass (g)	Test Mass	Mass (g)
M1	104.20 g	P3	39.13 g
M2	104.76 g	P4	39.07 g
M3	104.17 g	P5	40.52 g
M4	104.69 g	C1	10.62 g
M5	104.62 g	C2	7.76 g
P1	40.04 g	O1	213.85 g
P2	39.65 g	O2	228.35 g

16 distinct masses were calculated, making use of the ones above, approximately 50 g apart from each other, varying from 51.14 g to 812.64 g, as shown in the third column of Table 3. Multiplying the masses by the gravitational force obtained from CENEGEO, the mean force exerted by the motor can be estimated. Initially, 20 different test masses were calculated, with increments of approximately 50 g each. However, during the experiment with a mass of 855.21 g, the motor was unable to maintain stability with the optimized PID parameters. Even after increasing the proportional and derivative components to stabilize the rod, the actuator could not support masses of T17 and beyond, as the gravitational force exerted by these masses exceeded the actuator's capacity. Similarly, masses smaller than 39.07 g did not produce satisfactory current readings, as the force exerted was insufficient for the MCLM PID controller to precisely regulate position and speed, resulting in erratic signals. Therefore, it can be concluded that the effective mass range the actuator can handle is between 39.07 g and 812.64 g.

This conversion was possible because the only force exerted on the rod was the gravitational force applied by the masses attached to the rope. Subsequently, a calibration curve of the actual force exerted by the motor based on the apparent measured force was created by multiplying the current signal by the force constant shown in the LM 2070-080-11 linear motor, available on the manufacturer's website [22]. The flowchart for the protocol of data processing and calibration curve calculation is shown in Figure 8.

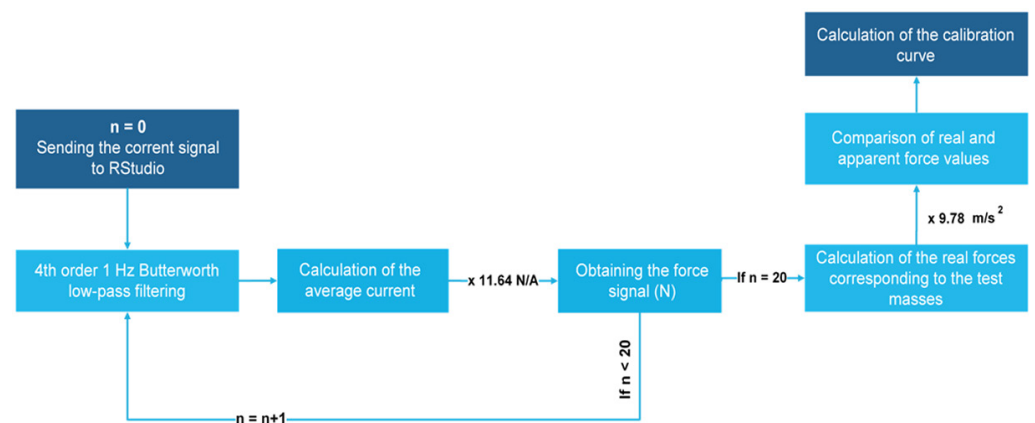


**Fig. 8.** Flowchart of the data collection protocol

### Protocol for calibrating the angular displacement caused by the orthosis.

To quantify the wrist's angular displacement caused by the actuator rod's movement, a goniometer was used. Similar to the force calculation, a calibration curve of wrist displacement in degrees was created based on the rod's incremental displacement, meaning each increment corresponds to a specific angular displacement. For the calibration, a GP10 goniometer and Myosystem-Br1 software were employed, using two protocols to create calibration curves [25]. For signal collection, the Myosystem-Br1 software, version 3.5.6 [26], was used to calibrate the 0-degree signal. This calibration aimed to set the 0-degree mark as close as possible to 0 in the obtained signal. However, due to a potentiometer shift when fixing the movable part to the fixed part, an offset appeared, which was digitally removed.

The goniometer was fixed to the orthosis so that the measured angle corresponded to the wrist's position angle, intending to calibrate the joint's angular displacement caused by the rod's movement. Due to anthropometric diversity, this positioning and calibration curve calculation must be done for each individual using the AWO. Different calibration protocols were considered for the calibration curve calculation. The first protocol involved capturing angular displacement and rod displacement signals for one minute at a 200 Hz sampling rate for values between  $-5,000$  and  $5,000$  increments, at every  $1,000$  increments. Thus, 11 angular displacement signals were obtained, sent to RStudio, and resampled to 166.67 Hz to compare both displacements. This resampling was done using the 'resamp()' function from the Seewave library in RStudio. The flowchart for this methodology is shown in Figure 9.

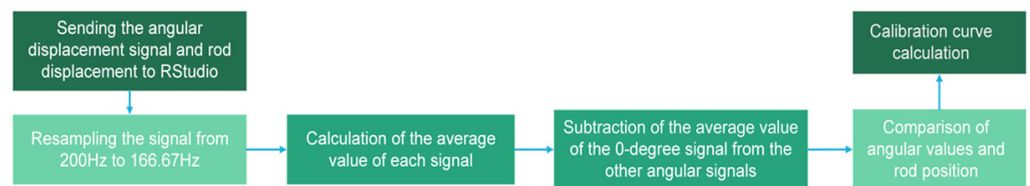


Fig. 9. Flowchart of Methodology 1 for angular displacement calibration

Because the rod displacement remained almost constant, the mean wrist angular displacement was calculated to obtain points relative to each thousand increments. Since the 0-degree value was not exactly at 0, the mean angular displacement value relative to 0 degrees was calculated and then subtracted from the other means, removing the preexisting offset. After calculating the means, they were plotted against the increments related to the angles, followed by a simple linear regression to establish a calibration curve of wrist angular displacement concerning the rod's displacement.

The second method for verifying angular displacement involved a routine executed in the Motion Manager 6 software, where the rod moved from the 0 position, varying between  $-5,000$  and  $5,000$  increments, at a speed of 50 increments per second for 90 seconds. This methodology considered that angular variations might not imply a change in rod position depending on their magnitude. Therefore, both the actuator displacement signals over time at a 166.67 Hz sampling rate and the goniometer signal at 200 Hz were captured simultaneously. To correct any lack of synchronism between the signals, they were synchronized in RStudio after collection. After resampling the goniometer signal from 200 to 166.67 Hz, the signals were synchronized, and the offset was removed. The offset removal

was performed similarly to the previous method: the mean angular values were calculated and then subtracted from all points of the angular displacement signal.

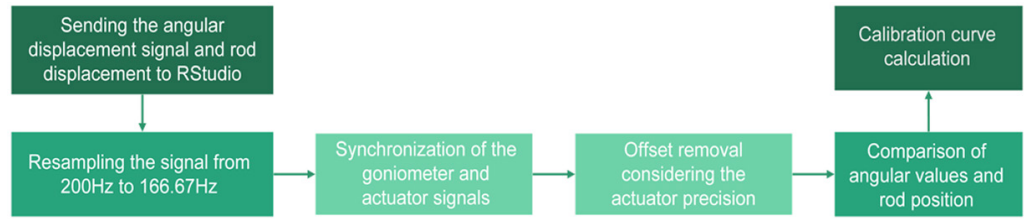


Fig. 10. Flowchart of Methodology 2 for angular displacement calibration

After removing the offset, a simple linear regression was calculated to obtain the calibration line of wrist angular displacement concerning the rod's displacement. The flowchart for Methodology 2 of angular displacement calibration is shown in Figure 10.

### 3 RESULTS

#### 3.1 Current signal evaluation

The current and position signals over time were captured at a sampling frequency of 166.67 Hz. One of the captured signals, corresponding to test mass T1 before filtering, is shown in Figure 11, with a mean current of 14.48 mA.

Since this is a DC (direct current) motor, its response is expected to be only in direct current, i.e., with a frequency close to zero. The pre-filtered spectrum shows a mean frequency of 18.97 Hz and a median frequency of 10.52 Hz. After filtering, changes were observed both in the time-domain signal and its power spectrum in the frequency domain. The respective frequency spectrum of the current signal from Figure 11.

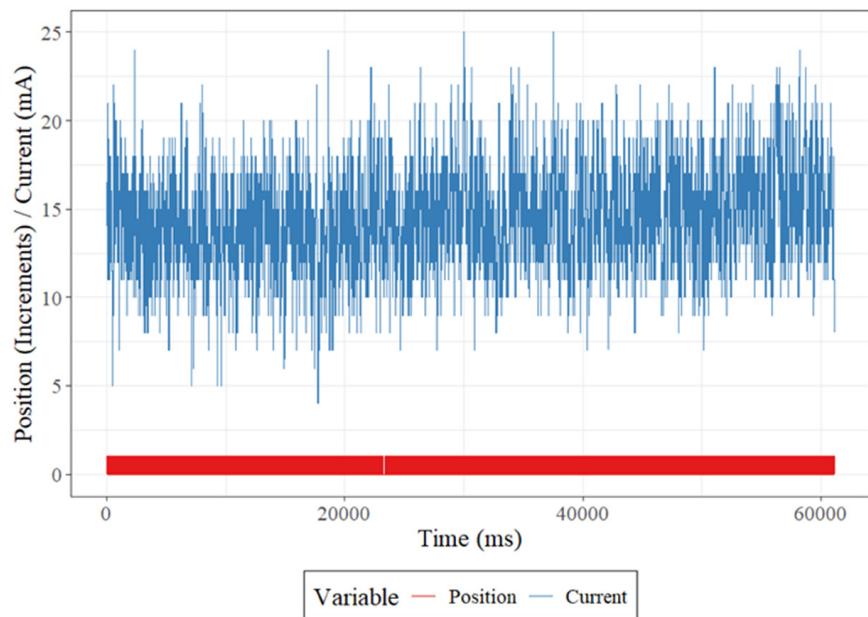


Fig. 11. Current signal and rod position over time for mass T1

It is noted that higher frequency oscillations were cut from the current signal in the time domain, leaving practically the mean of 14.06 mA, a 2.9% decrease from the original value. The mean and median frequencies decreased to 6.9 Hz and 0.15 Hz, respectively, with percentage decreases of 63.42% and 98.67%, respectively. This indicates that the filtering procedure had a greater impact on the variables analyzed in the frequency domain, as expected since most of the signal's energy is concentrated at 0 Hz.

### 3.2 Force signal calibration

According to the proposed methodology, the mean current values were first calculated over a stipulated time window of 60 seconds after applying a fourth-order 1 Hz low-pass Butterworth filter to the signal. These values were then multiplied by 11.64 N/A, as specified in the actuator's technical manual [22]. Initially, 20 test masses were calculated. However, during the experiment with mass T17, the motor could not maintain balance with the optimized PID parameters. Even after increasing the proportional and derivative components of the position to try to keep the rod stationary, it was impossible to hold masses T17 and beyond, as the gravitational force exerted by them was greater than what the actuator could support.

Similarly, masses less than 39.07 g did not produce satisfactory current results since the mass did not exert enough force for the MCLM PID controller to accurately regulate position and speed, resulting in erratic signals. Thus, the range of mass that the actuator can move is from 39.07 g to 812.64 g. Adding lateral rods could provide more stability to the moveable rod and help dissipate the load force among them, potentially increasing this range. However, a new calibration curve calculation considering the entire system would be necessary. Therefore, the mean current values found for each test mass from 1 to 16 and the corresponding force for each are shown in Table 2.

**Table 2.** Mean current and force values calculated after filtering

Test Mass	Mean Current	Mean Force	Apparent Mass
T1	14.06 mA	0.16 N	16.36 g
T2	70.14 mA	0.82 N	83.84 g
T3	104.71 mA	1.22 N	124.74 g
T4	154.33 mA	1.80 N	184.05 g
T5	198.02 mA	2.30 N	235.17 g
T6	229.99 mA	2.68 N	274.03 g
T7	272.02 mA	3.17 N	324.13 g
T8	320.33 mA	3.73 N	381.39 g
T9	362.71 mA	4.22 N	431.49 g
T10	397.88 mA	4.63 N	473.42 g
T11	448.19 mA	5.22 N	533.74 g

*(Continued)*

**Table 2.** Mean current and force values calculated after filtering (*Continued*)

Test Mass	Mean Current	Mean Force	Apparent Mass
T12	484.22 mA	5.64 N	576.69 g
T13	525.84 mA	6.12 N	625.77 g
T14	586.11 mA	6.82 N	697.34 g
T15	626.56 mA	7.29 N	745.40 g
T16	656.79 mA	7.65 N	782.21 g

Table 3 presents the result of the comparison between real mass and force and measured mass and force, as well as the accuracy of the measurement made by the software and the actual constant between the measured current and the real force.

**Table 3.** Real and apparent masses and forces, the accuracy of the measurement conducted, and the real force constant calculated for each measurement

Test Mass	Apparent Mass	Real Mass	Apparent Force	Real Force	Accuracy of the Measure	Real Constant
T1	16.31 g	51.14 g	0.16 N	0.50 N	32.00%	35.76 N/A
T2	83.62 g	114.79 g	0.82 N	1.13 N	72.56%	16.09 N/A
T3	124.74 g	153.89 g	1.22 N	1.51 N	80.79%	14.45 N/A
T4	184.05 g	218.99 g	1.80 N	2.15 N	83.72%	13.95 N/A
T5	235.17 g	259.51 g	2.30 N	2.55 N	90.20%	12.88 N/A
T6	274.03 g	300.11 g	2.68 N	2.95 N	90.85%	12.83 N/A
T7	324.13 g	351.49 g	3.17 N	3.46 N	91.62%	12.70 N/A
T8	381.39 g	407.43 g	3.73 N	4.01 N	93.02%	12.50 N/A
T9	431.49 g	455.10 g	4.22 N	4.47 N	94.41%	12.33 N/A
T10	473.42 g	501.10 g	4.63 N	4.93 N	93.91%	12.38 N/A
T11	533.74 g	559.79 g	5.22 N	5.50 N	94.91%	12.28 N/A
T12	576.69 g	605.27 g	5.64 N	5.95 N	94.79%	12.29 N/A
T13	625.77 g	650.05 g	6.12 N	6.39 N	95.77%	12.15 N/A
T14	697.34 g	708.61 g	6.82 N	6.97 N	97.85%	11.88 N/A
T15	745.40 g	754.67 g	7.29 N	7.42 N	98.24%	11.84 N/A
T16	782.21 g	812.64 g	7.65 N	7.99 N	95.74%	12.16 N/A

The approximate force constant that should be used to estimate the force exerted by the motor based on its current consumption is the mean of the force constants obtained for each point: 14.28 N/A. There is an 18.49% difference between the provided and calculated force constants.

It is observed that both forces follow a similar growth pattern. To establish a direct relationship between the two forces and calculate the real force based on the measured force, a simple linear regression was first performed (with the real force estimated by the apparent force) between the forces. The result of this regression is shown in Figure 12.

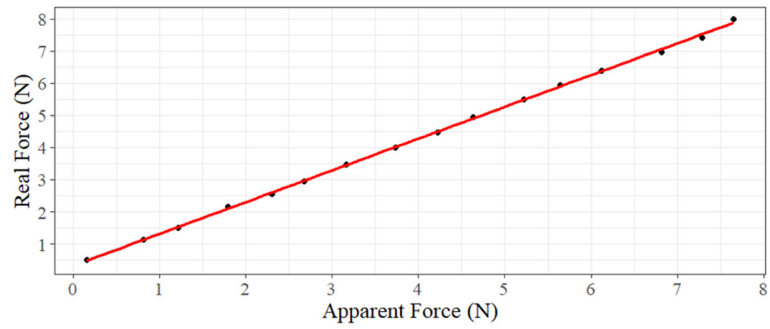


**Fig. 12.** Linear regression between real force and apparent force

Considering a 95% confidence interval, the p-value of the apparent force is less than  $10^{-16}$ , indicating that changes in this variable cause statistically significant changes in the response variable, the real force. The equation of the adjusted regression line is represented in Equation 1.

$$Real\ Force = 0.33 + 0.99 \times (Apparent\ Force) \tag{1}$$

This means that for every 1 N change in the apparent force detected by the software, there is an estimated increase of 0.99 N in the real force. The Pearson correlation coefficient found is 0.9997189. By applying Equation 1 to the apparent force data in Table 2, the accuracy of the obtained equation can be estimated. The accuracy fluctuates between 98% for the smallest mass and 100% for two of the largest masses, with the mean accuracy being 98.94% and a Pearson correlation coefficient between the real and calculated force values of 0.9997298. These results corroborate the validity of applying the obtained equation to the apparent values captured via Motion Manager.

### 3.3 Calibration of wrist angular displacement

**Methodology 1 for angular displacement calibration.** Following the first proposed methodology, the goniometer signals, corresponding to each specific increment, are shown in Figure 13. These signals have been resampled to a frequency of 166.67 Hz.

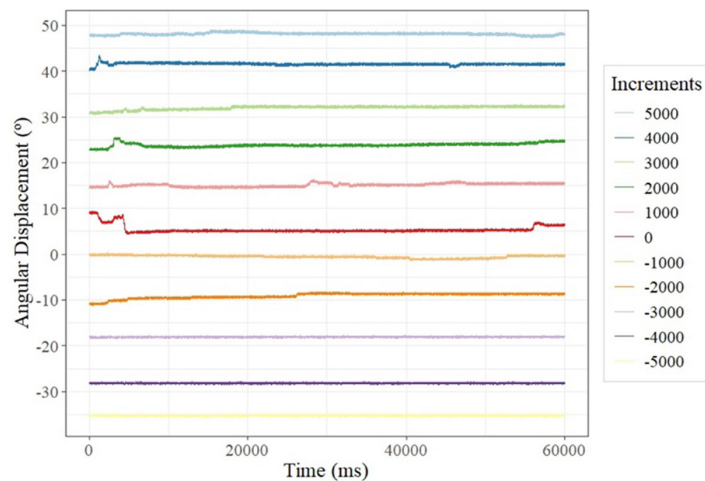


**Fig. 13.** Goniometer’s signals

By measuring the angles and the position of the rod in increments, a relationship between them can be established. Plotting the angle values on the Y-axis and the increments on the X-axis, a linear relationship is evident. A simple linear regression was used to estimate an equation that relates these values. The regression line is presented in Figure 14.

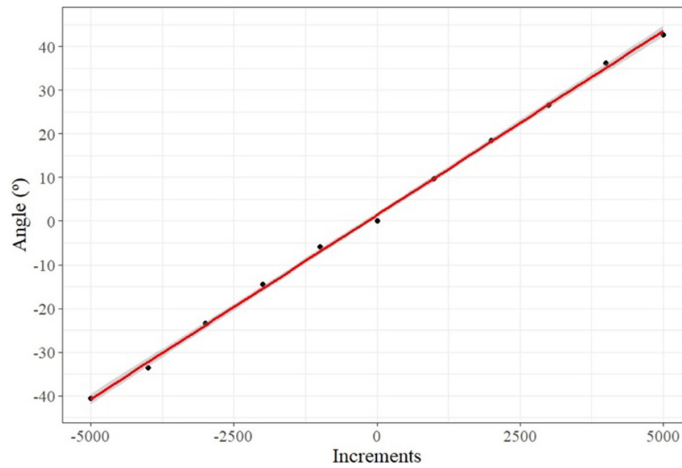


**Fig. 14.** Linear regression between wrist angular displacement and actuator position

Considering a 95% confidence interval, the p-value of the increments is less than  $10^{-16}$ , indicating that changes in this variable cause statistically significant changes in the response variable, which is the wrist angular displacement. The equation of the fitted regression line is represented in Equation 2.

$$Angle = 1.41 + 8.44 \times 10^{-3} \times (Increment) \tag{2}$$

This means that for every 1000 increments traveled by the rod, there would be an increase of  $8.44^\circ$  in the wrist angle. The Pearson correlation coefficient found is 0.9995091.

**Methodology 2 for angular displacement calibration.** The signals collected by the Motion Manager and myosystem were processed using RStudio software and was observed that the signals were not yet synchronized. Therefore, synchronization was done using the peaks of both signals as a reference. A difference of 2394 ms between the peaks of the signals was found. After synchronization, the result can be seen in Figure 15.

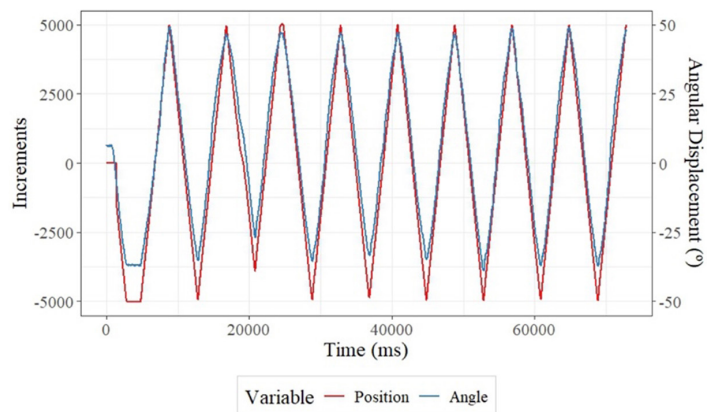


**Fig. 15.** Synchronization of rod displacement signals and wrist angular displacement

However, the angular signal offset was still present. The mean angular displacement signal was  $5.463^\circ$ . This mean was subtracted from all points of the angular signal, and a linear model was then created between the analyzed signals. The equation of the fitted regression line is represented in Equation 3.

$$\text{Angle} = 0.6 + 9.08 \times 10^{-3} \times (\text{Increment}) \quad (3)$$

For every 1000 increments traveled by the rod, there would be an increase of  $9.08^\circ$  in the wrist angle. The Pearson correlation coefficient found is 0.995259.

## 4 DISCUSSION

The research conducted for this dissertation aimed to validate the use of an active wrist orthosis developed at NIATS for quantifying rigidity in patients with PD. Precise and relevant feature extraction necessitates rigorous calibration of the force and angular displacement signals of the wrist. Due to the manufacturing process of the MCLM 3006 S RS controller and the LM 2070-080-11 actuator, initial attempts to measure the motor's current accurately were unsuccessful. However, by connecting an ammeter to the circuit's battery output, similar current values to those in Table 2 were observed. Despite not being a valid method for calibrating the current signal obtained by the motion manager, the graphical analysis tool's results were trusted due to their proximity to the expected values.

For calibrating the force signals exerted by the actuator, several challenges were encountered. Without any load on the rod, erratic current signals appeared, especially when touched. These currents were attributed to the MCLM PID controller, which should not consume current without effective movement. Tests showed that the current values from the Motion Manager are unreliable if the motor is connected to little or no mass. Therefore, methods that keep the actuator stationary for long periods can cause current measurement issues. Better hand fixation to the support is needed to apply constant force to the motor. However, during rigidity analysis in PD patients, continuous forces are expected throughout the data collection protocol.

High-frequency filtering ( $>1$  Hz) was performed to minimize artifacts such as cable movement. The results showed minimal impact in the time domain but significant changes in the frequency domain, as indicated by the percentage decreases in the analyzed variables during the current verification. This filtering may not be necessary, as most signal energy is at 0 Hz, consistent with DC motor signals. However, high-frequency artifacts or noise may appear in the signal; thus, filtering is recommended to avoid these issues. Given that this research focuses on PD, known for causing tremors, low-pass filtering at 1 Hz would help remove movements due to Parkinsonian tremors, which typically have frequencies between 4 and 6 Hz.

Regarding the range of mass that the actuator can support (39.07 g to 812.64 g), it is theoretically possible to increase this range by reinforcing the part connected to the actuator. The relative mass of the human hand is estimated to be 0.61% of the total mass of males and 0.56% of the total mass of females. The mean mass of the Brazilian population is 73 kg for men and 63 kg for women, respectively [21]. Assuming an equal distribution between genders, the mean mass of the hands to be moved is 399 g. Considering that the entire hand mass will be moved (despite force decomposition; this is considered the "worst case" for the actuator) by the motor and taking the gravitational acceleration as  $9.83 \text{ m/s}^2$  [24], there is a constant force of 3.92 N pulling the hand down. According to the calibration performed in this work, even if rigidity should theoretically double the required force for the actuator to perform the proposed movement, it would still be possible to do so.

Statistical metrics related to the force calibration results ( $R > 0.99$ ) reinforce the validity of the method employed, despite potential adjustments or improvements that may be made to refine the methodology applied here.

For angular displacement calibration, a protocol was established to directly quantify wrist angular displacement based on rod displacement, eliminating the angle between the rod and the spherical joint system that allows multidimensional hand movement. Two calibration curves were determined due to differences in experimental protocols. The second angular analysis methodology showed a smaller intercept ( $0.6$  compared to  $1.41$ ) but a larger position coefficient ( $9.08 \times 10^{-3}$  compared to  $8.44 \times 10^{-3}$ ). This difference may have occurred due to the greater stability of the MCLM 3006 S RS PID controller during continuous movement, as previously discussed.

For wrist angular displacement, the first calibration curve is recommended for protocols with the rod stationary for a period, while the second curve is recommended for continuous movement protocols. Both methodologies showed high Pearson correlation values ( $R > 0.99$ ) indicating their validity, despite potential adjustments or improvements that may be needed.

To ensure the generalizability of the results presented here, a larger-scale study is necessary, preferably involving both healthy individuals and patients with Parkinson's disease.

Regarding clinical implementation, the primary cost is associated with the materials used, specifically the motor and controller, as these are the most expensive components. Once implemented, clinicians would be able to capture data from which valuable information could be extracted, such as RMS values, average frequency, and the current consumed during movement. This data would provide relevant insights into the stiffness present in the wrist joint. To facilitate patient acceptance, the orthosis was designed using comfortable and lightweight materials, as described in [20].

## 5 CONCLUSION

For the present study, the force exerted by the motor related to the current it consumes and the angular displacement of the wrist caused by the movement of the actuator rod were calibrated, achieving the proposed objectives. In a practical application where the orthosis is positioned on an individual's forearm, anthropometric data can be used to construct a rigid body system, decomposing the force exerted by the motor according to the angles between the orthosis parts and the individual's body. This allows for the estimation of the torque applied to the wrist joint.

Following this analysis, which uses anthropometric data, the obtained calibration curves can be improved by considering these data and adding them as new variables to the line. This makes it possible to determine both the angular displacement of the wrist and the force applied to the hand or the torque applied to the wrist joint based on these values. For this, an optimal position of the orthosis should be considered. Such standardization allows for the addition of new variables if a rigid body system is considered, as mentioned earlier. For future work, it is worth noting the possibility of using artificial intelligence tools, such as machine learning algorithms, for optimizing the PID controller parameters, potentially improving the results, especially concerning current consumption relative to the displacement of the rod.

For the quantification of rigidity in patients with PD, it is expected to extract various signal characteristics, such as the force exerted by the motor about the angular displacement of the wrist or the current consumed by the motor over time, similar

to what was presented in [16]. This underscores the relevance of the research presented here, as precise and reliable data capable of producing highly reliable results require calibration.

This rigor, employed in the proposed methodology, along with the obtained results, reinforces the validity of the procedures used. Consequently, this work enables the use of this method for a potential new scale of rigidity quantification, which is highly relevant for providing more objectivity in quantifying rigidity in patients with Parkinson's disease.

## 6 ACKNOWLEDGMENTS

The authors of this work are grateful to the National Council for Scientific and Technological Development (CNPq); the Coordination for the Improvement for Higher Level Personnel (CAPES); the Ministry of Science, Technology, Innovation, and Communications (MCTIC); the Research Foundation of the State of Minas Gerais (FAPEMIG); the Instituto Federal de Educação, Ciência e Tecnologia Goiano (IF Goiano) – Campus Cristalina and Campus Rio Verde, for the financial and structural support to conduct this study. A. A. Pereira is a research productivity fellow at CNPq, Brazil.

## 7 REFERENCES

- [1] S. Cerri, L. Mus, and F. Blandini, "Parkinson's disease in women and men: What's the difference?" *J. Parkinsons Dis.*, vol. 9, no. 3, pp. 501–515, 2019. <https://doi.org/10.3233/JPD-191683>
- [2] J. Jankovic, "Parkinson's disease: Clinical features and diagnosis," *Journal of Neurology, Neurosurgery and Psychiatry*, vol. 79, no. 4, 2008. <https://doi.org/10.1136/jnnp.2007.131045>
- [3] M. J. Kwon, J.-H. Kim, J. H. Kim, S. J. Cho, E. S. Nam, and H. G. Choi, "The occurrence of Alzheimer's disease and Parkinson's disease in individuals with osteoporosis: A longitudinal follow-up study using a national health screening database in Korea," *Front. Aging Neurosci.*, vol. 13, 2021. <https://doi.org/10.3389/fnagi.2021.786337>
- [4] C. G. Goetz *et al.*, "Movement disorder society-sponsored revision of the unified Parkinson's disease rating scale (MDS-UPDRS): Scale presentation and clinimetric testing results," *Movement Disorders*, vol. 23, no. 15, pp. 2129–2170, 2008. <https://doi.org/10.1002/mds.22340>
- [5] X. Wen, Z. Liu, X. Liu, Y. Peng, and H. Liu, "The effects of physiotherapy treatments on dysphagia in Parkinson's disease: A systematic review of randomized controlled trials," *Brain Res. Bull.*, vol. 188, pp. 59–66, 2022. <https://doi.org/10.1016/j.brainresbull.2022.07.016>
- [6] K. L. K. Au *et al.*, "A randomized clinical trial of burst vs. spaced physical therapy for Parkinson's disease," *Parkinsonism Relat. Disord.*, vol. 97, pp. 57–62, 2022. <https://doi.org/10.1016/j.parkreldis.2022.02.021>
- [7] A. Esquenazi and M. Talaty, "Robotics for lower limb rehabilitation," *Phys. Med. Rehabil. Clin. N. Am.*, vol. 30, no. 2, pp. 385–397, 2019. <https://doi.org/10.1016/j.pmr.2018.12.012>
- [8] X. Huang, F. Naghdy, G. Naghdy, H. Du, and C. Todd, "The combined effects of adaptive control and virtual reality on robot-assisted fine hand motion rehabilitation in chronic stroke patients: A case study," *Journal of Stroke and Cerebrovascular Diseases*, vol. 27, no. 1, pp. 221–228, 2018. <https://doi.org/10.1016/j.jstrokecerebrovasdis.2017.08.027>

- [9] R. J. Varghese, D. Freer, F. Deligianni, J. Liu, and G.-Z. Yang, "Wearable robotics for upper-limb rehabilitation and assistance," *Wearable Technology in Medicine and Health Care*, Elsevier, pp. 23–69, 2018. <https://doi.org/10.1016/B978-0-12-811810-8.00003-8>
- [10] X. Xue, X. Yang, and Z. Deng, "Efficacy of rehabilitation robot-assisted gait training on lower extremity dyskinesia in patients with Parkinson's disease: A systematic review and meta-analysis," *Ageing Res. Rev.*, vol. 85, p. 101837, 2023. <https://doi.org/10.1016/j.arr.2022.101837>
- [11] A. Berardi *et al.*, "Tools to assess the quality of life in patients with Parkinson's disease: A systematic review," *Expert Rev Pharmacoecon Outcomes Res.*, vol. 21, no. 1, pp. 55–68, 2021. <https://doi.org/10.1080/14737167.2021.1841638>
- [12] B. Lacy, H. J. Piotrowski, R. B. Dewey, and M. M. Husain, "Severity of depressive and motor symptoms impacts quality of life in Parkinson's disease patients at an academic movement clinic: A cross-sectional study," *Clin. Park. Relat. Disord.*, vol. 8, p. 100180, 2023. <https://doi.org/10.1016/j.prdoa.2022.100180>
- [13] M. D. R. Ferreira-sánchez, M. Moreno-verdú, and R. Cano-de-la-cuerda, "Quantitative measurement of rigidity in Parkinson's disease: A systematic review," *Sensors*, vol. 20, no. 3, p. 880, 2020. <https://doi.org/10.3390/s20030880>
- [14] J. Gao *et al.*, "Ultrasound strain elastography in assessment of resting biceps brachii muscle stiffness in patients with Parkinson's disease: A primary observation," *Clinical Imaging*, vol. 40, no. 3, pp. 440–444, 2016. <https://doi.org/10.1016/j.clinimag.2015.12.008>
- [15] E. A. Shamim, J. Chu, L. H. Scheider, J. Savitt, H. A. Jinnah, and M. Hallett, "Extreme task specificity in writer's cramp," *Movement Disorders*, vol. 26, no. 11, pp. 2107–2109, 2011. <https://doi.org/10.1002/mds.23827>
- [16] T. Perera *et al.*, "A palm-worn device to quantify rigidity in Parkinson's disease," *Journal of Neuroscience Methods*, vol. 317, pp. 113–120, 2019. <https://doi.org/10.1016/j.jneumeth.2019.02.006>
- [17] P. Gapielian, S. H. Scott, C. Lowrey, S. Reid, G. Pari, and R. Levy, "Integrated robotics platform with haptic control differentiates subjects with Parkinson's disease from controls and quantifies the motor effects of levodopa," *J. Neuroeng. Rehabil.*, 2019. <https://doi.org/10.1186/s12984-019-0598-5>
- [18] A. M. Bruder, N. F. Taylor, K. J. Dodd, and N. Shields, "Physiotherapy intervention practice patterns used in rehabilitation after distal radial fracture," *Physiotherapy*, vol. 99, no. 3, pp. 233–240, 2013. <https://doi.org/10.1016/j.physio.2012.09.003>
- [19] M. Mitsukane, N. Sekiya, S. Himeji, and K. Oyama, "Immediate effects of repetitive wrist extension on grip strength in patients with distal radial fracture," *Archives of Physical Medicine and Rehabilitation*, vol. 96, no. 5, pp. 862–868, 2015. <https://doi.org/10.1016/j.apmr.2014.09.024>
- [20] S. C. Costa and A. de O. Andrade, "Avaliação ergonômica de uma órtese ativa de punho para a reabilitação da rigidez em pessoas com a doença de parkinson," *Universidade Federal de Uberlândia*, 2020.
- [21] A. O. Andrade, J. Bourget, S. Costa, A. Pereira, M. I. Okereke, and M. F. Vieira, "Ergonomic assessment of an active orthosis for the rehabilitation of flexion and extension of wrist," in *World Congress on Medical Physics and Biomedical Engineering 2018*, 2019, pp. 565–568. [https://doi.org/10.1007/978-981-10-9038-7\\_104](https://doi.org/10.1007/978-981-10-9038-7_104)
- [22] FAULHABER, "Technical Manual – Linear DC-Servomotors," 2023.
- [23] FAULHABER, "Datasheet Motion Controllers V2.5," 2023.
- [24] CENEGEO, "Referência Gravimétrica da cidade de Uberlândia," 2020.
- [25] DATA HOMINIS, "Myosystem-BR1 P84," Uberlândia, 2016.
- [26] DATA HOMINIS, "Software Myosystem-BR1," Uberlândia, 2016.

## 8 AUTHORS

**Caio Tonus Ribeiro** is a student of the Postgraduate Program in Biomedical Engineering at the Faculty of Electrical Engineering, Federal University of Uberlândia, Minas Gerais, Brazil (E-mail: [caiot@ufu.br](mailto:caiot@ufu.br)).

**Daniel Hilário da Silva** is a student of the Postgraduate Program in Biomedical Engineering, at the Faculty of Electrical Engineering, Federal University of Uberlândia, and is working as a Lecturer at the Instituto Federal de Educação, Ciência e Tecnologia Goiano – Campus Cristalina, Goiás, Brazil (E-mail: [daniel.hilario@ifgoiano.edu.br](mailto:daniel.hilario@ifgoiano.edu.br)).

**Leandro Rodrigues da Silva Souza** is a student of the Postgraduate Program in Biomedical Engineering at the Faculty of Electrical Engineering, Federal University of Uberlândia, and is working as a Lecturer at the Instituto Federal de Educação, Ciência e Tecnologia Goiano, Campus Rio Verde, Goiás, Brazil (E-mail: [leandro.souza@ifgoiano.edu.br](mailto:leandro.souza@ifgoiano.edu.br)).

**José Renato Munari Nardo** is a student of the Postgraduate Program in Biomedical Engineering, at the Faculty of Electrical Engineering, Federal University of Uberlândia, Minas Gerais, Brazil (E-mail: [jose.munari@ufu.br](mailto:jose.munari@ufu.br)).

**Adriano Alves Pereira** is a Professor in the Postgraduate Program in Biomedical Engineering at the Faculty of Electrical Engineering, Federal University of Uberlândia, Minas Gerais, Brazil (E-mail: [adriano.pereira@ufu.br](mailto:adriano.pereira@ufu.br)).